Supporting information

Superhydrophobic and elastic silica/polyimide aerogel based on double confinement growth strategy of the co-sol system

Zhou Xiao,[†] Jing Che[†], Huaxin Li, [†] Xian Yue, [‡] Xianbo Yu, [†] Fenglei Sun, [†] Chao Xue[†] and Junhui Xiang[†]*

[†] Center of Materials Science and Optoelectronics technology, College of Materials Sciences and Optoelectronics technology, University of Chinese Academy of Sciences, Beijing, 100049, People's Republic of China.

[‡] School of Energy and Environment, City University of Hong Kong, Hong Kong 999077, China.

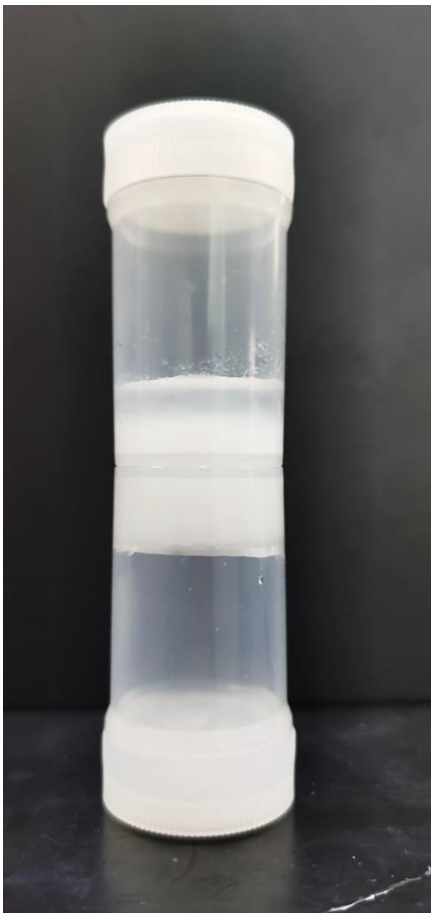

Fig. S1 The presence or absence of PAAs affects the gelation of MTMS in a pure water solvent system. The container below is a uniform gel formed by mixing TEA aqueous solution of PAAs and MTMS hydrolysate. The container above is a layered system formed by mixing TEA aqueous solution and MTMS hydrolysate. The TEA concentration and MTMS concentration in the two containers are the same.

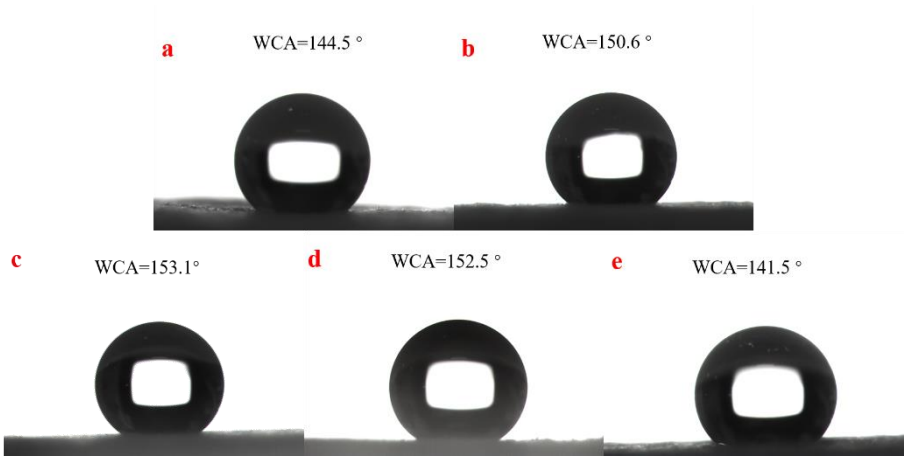

Fig. S2 The water contact angle (WCA) of aerogels. (a) SiO_2/PI-2. (b) SiO_2/PI-10. (c) SiO_2/PI-30. (d) SiO_2/PI-D. (e) SiO_2/PI-ND.

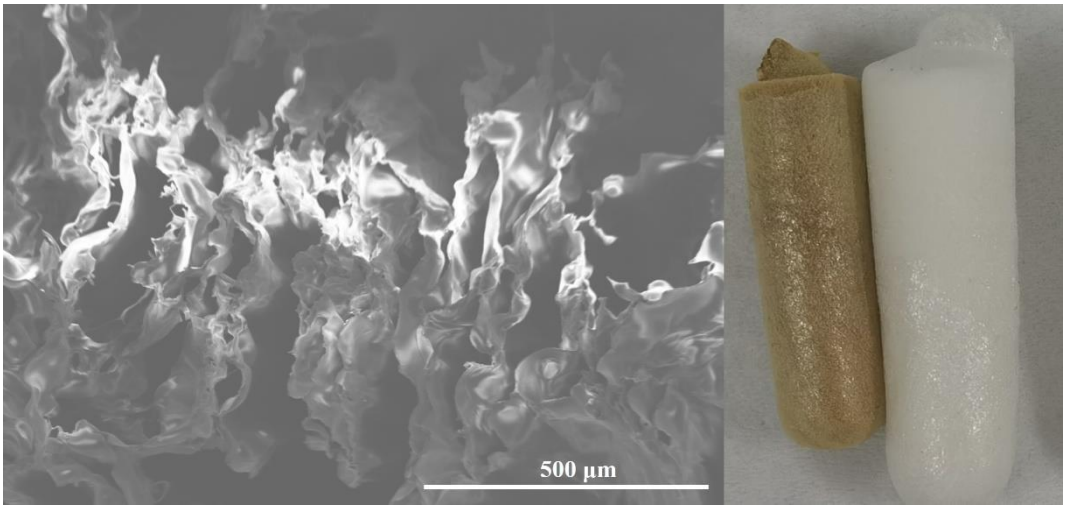

Fig. S3 Pure PI aerogel has a significant curling of the wall structure after thermal imidization. The volume of the aerogel shrinks significantly.

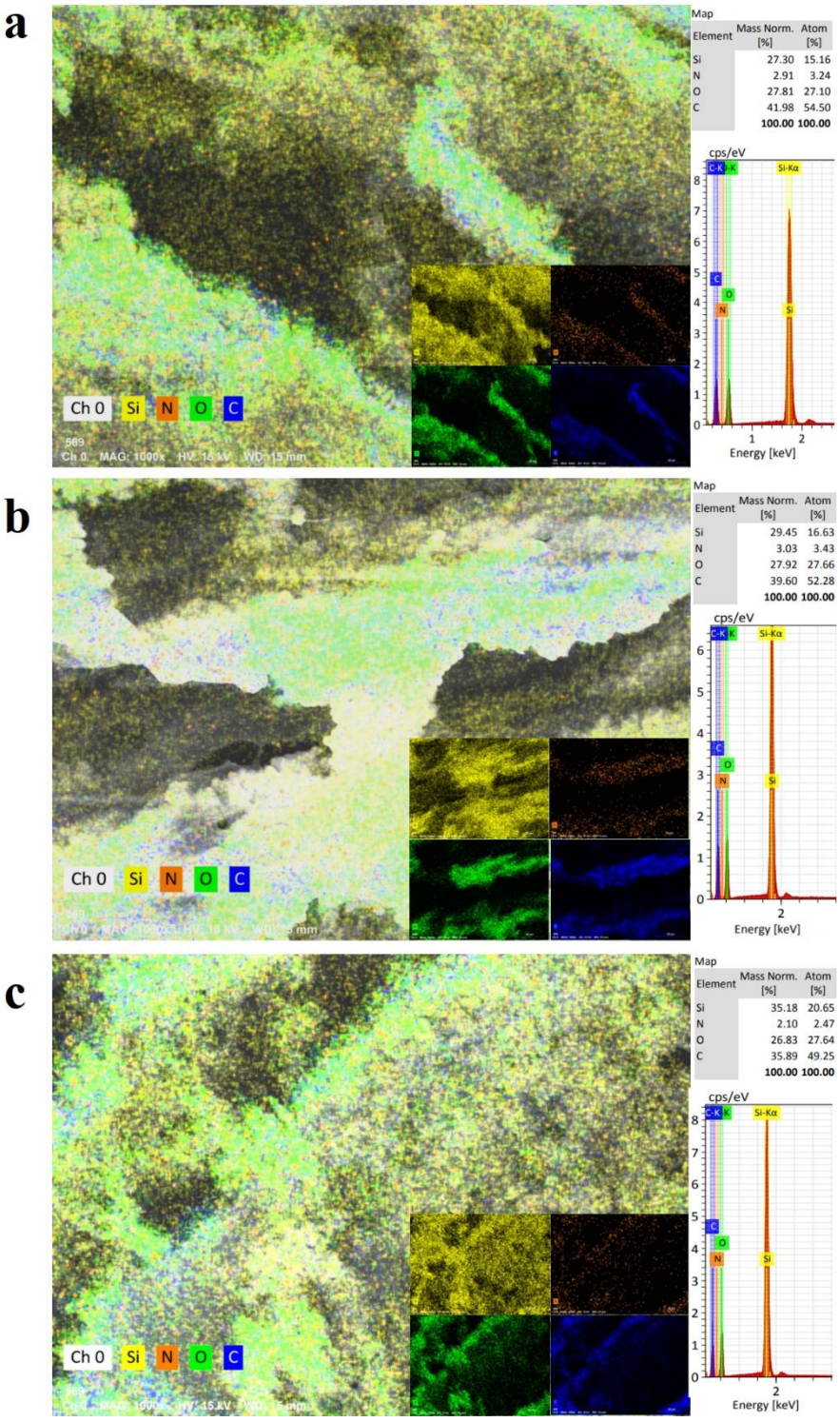

Fig. S4 EDS spectrum and element content table of (a) SiO_2/PI-2, (b) SiO_2/PI-10 and (c) SiO_2/PI-D.

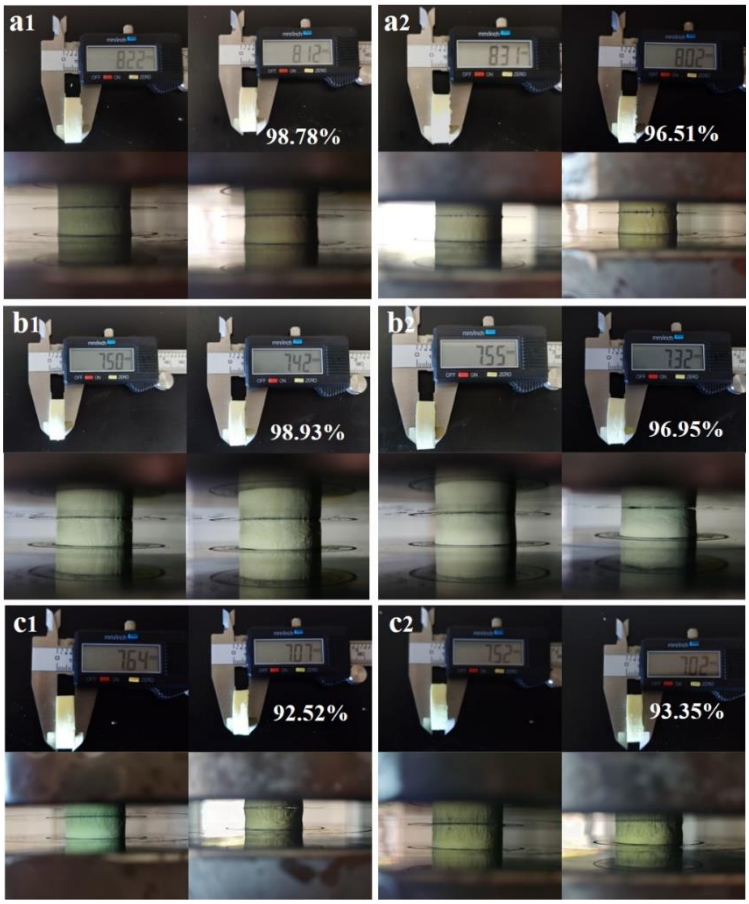

Fig. S5 The comparison photo before and after compression of (a) SiO_2/PI-2. (b) SiO_2/PI-30. (c) SiO_2/PI-ND. (1) Compression with 80% strain. (2) Compression with 50% strain for 50 consecutive times.

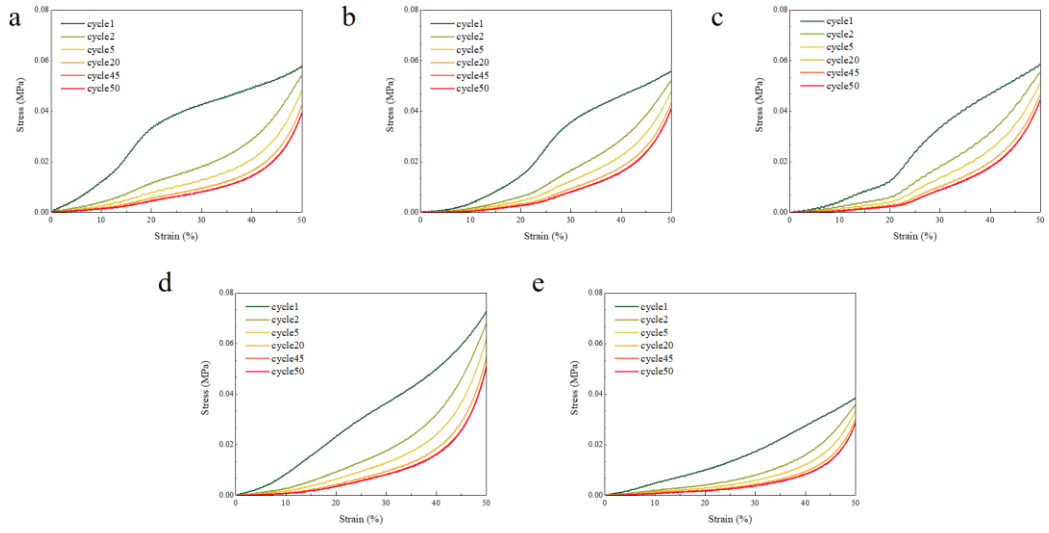

Fig. S6 The stress-strain curve at 50% strain with 50 cycles. (a) SiO_2/PI-2. (b) SiO_2/PI-10. (c) SiO_2/PI-30. (d) SiO_2/PI-D. (e) SiO_2/PI-ND.

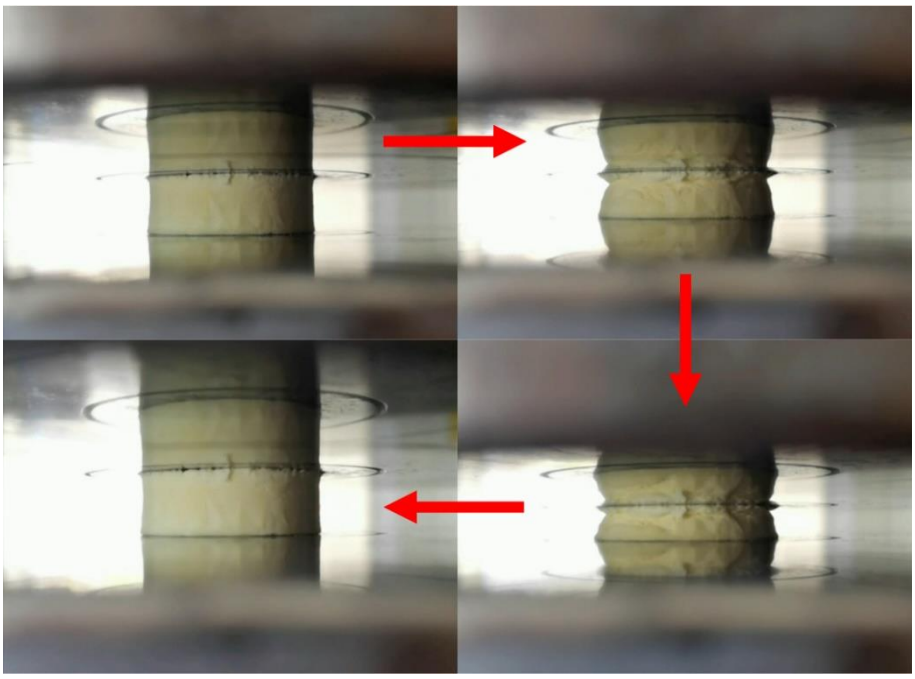

Fig. S7 The press-release process photograph of aerogels.

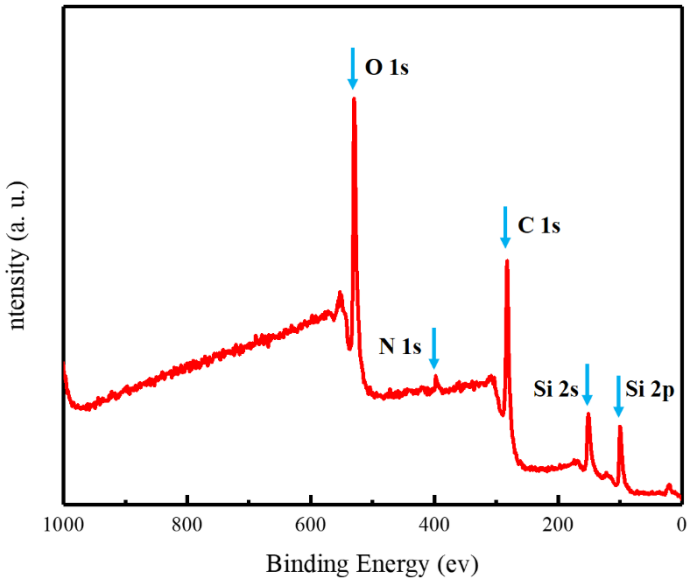

Fig. S8 XPS spectra of SiO_2/PI-10.

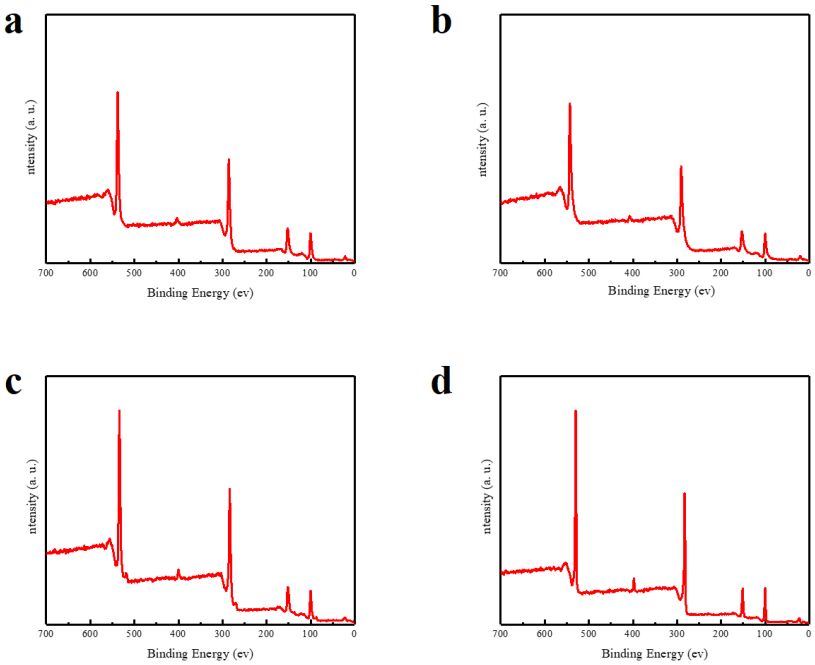

Fig. S9 XPS spectra of (a) SiO_2/PI-2. (b) SiO_2/PI-30. (c) SiO_2/PI-D. (d) SiO_2/PI-ND.

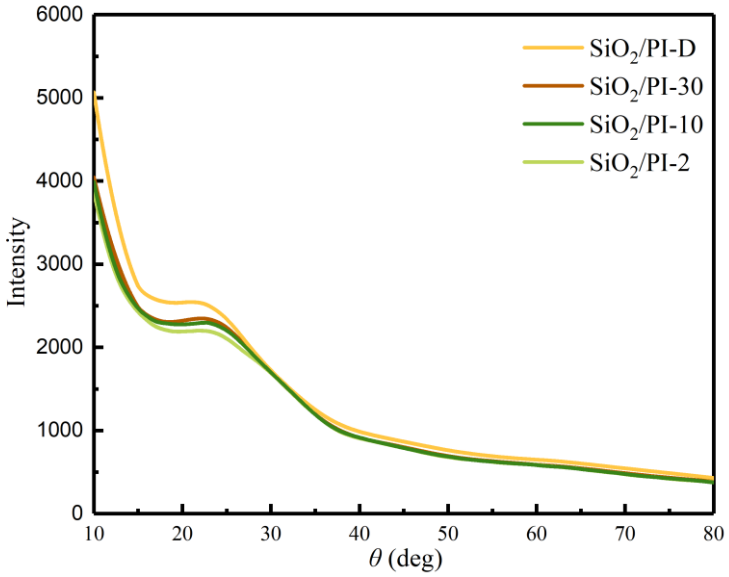

Fig. S10 XRD spectra of SiO_2/PI aerogels at different mixing times.

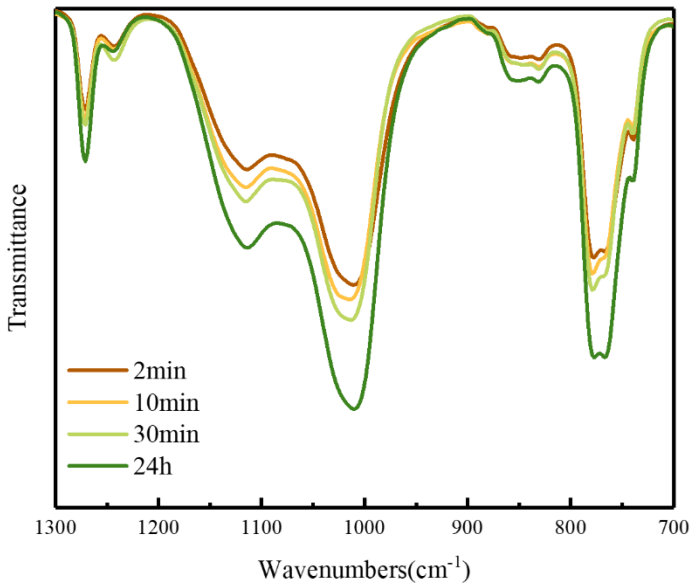

Fig. S11 Partial magnified FTIR spectra of SiO_2/PI aerogels at different mixing times.

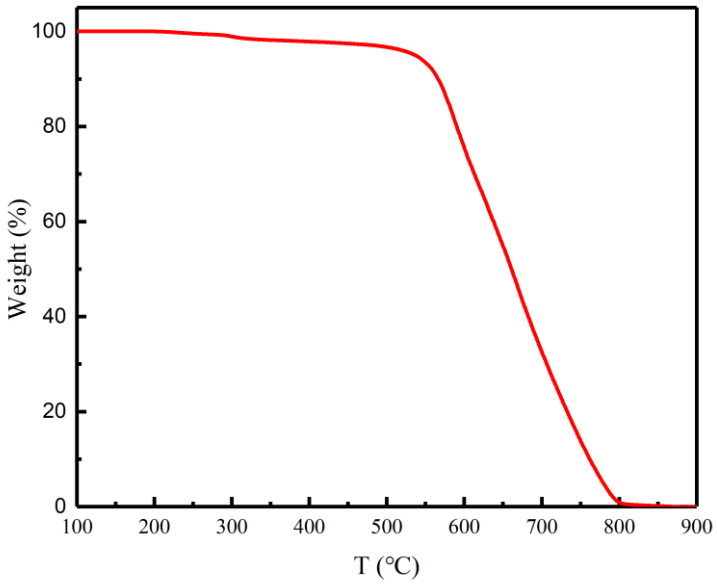

Fig. S12 TGA curve of pure PI aerogel in air atmosphere.

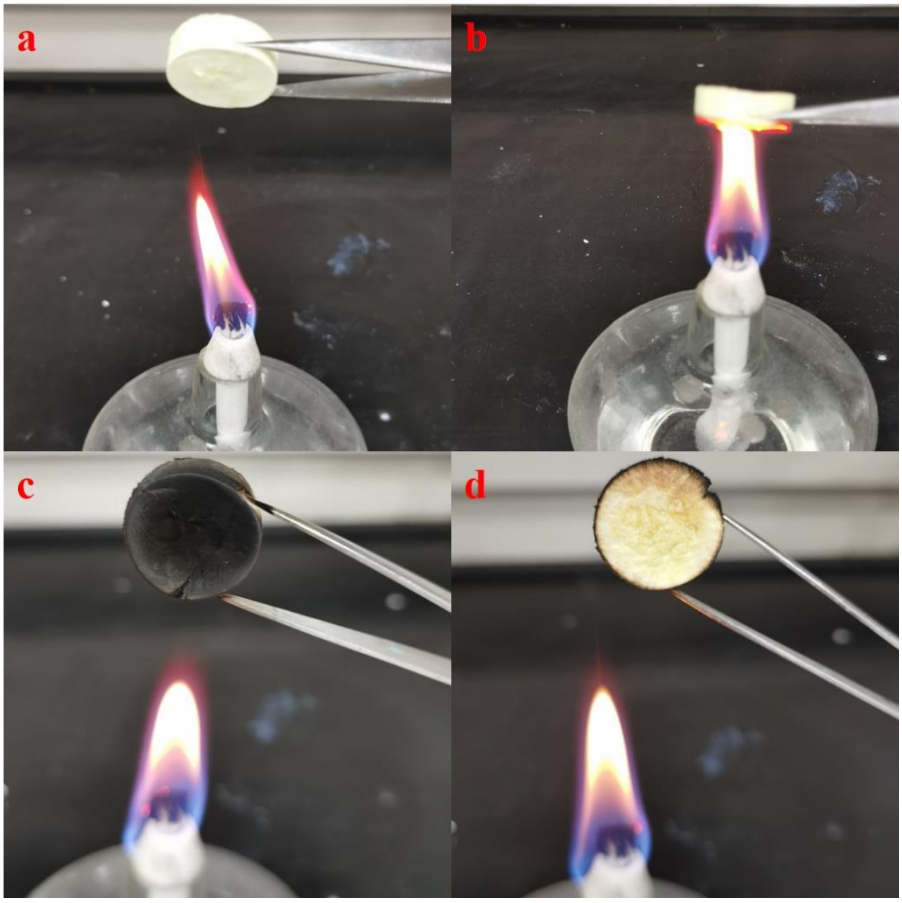

Fig. S13 The SiO_2/PI-10 aerogel burns under the flame. (a) SiO_2/PI-10 aerogel before burning. (b) Aerogel does not burn on the flame. (c) The burning surface of the aerogel is carbonized. (d) The side opposite to the burning side of the aerogel was not affected by the flame.

Table S1 The properties of elastic aerogels and hydrophobic aerogels have been reported.

Sample	Recovery rate (%)	WCA (°)	k ($W \cdot m^{-1} \cdot K^{-1}$)	Dry	T_d (℃)	Ref.
PINFAs	Without obvious plastic (99% strain)	~	0.030-0.032	Electrospinning & freeze drying	520.0 (air)	1
PI-PVPMS	80% (60% strain)	~	0.036-0.078	Supercritical drying	400.0 (air)	2
PINF/MXene	98.45% (50% strain)	122.5-127.5	~	Freeze drying	476.0 (air)	3
PI/ MWNTs	Without obvious plastic (50% strain)	~	~	Freeze drying	~	4
MXene/PI	without obvious plastic (80% strain)	~	0.032	Freeze drying	460.0 (air)	5
PEDOT:PSS/PI	Without obvious plastic (80% strain)	~	~	Freeze drying	350 (N_2)	6
PI/rGO/Co	97.8% (50% strain)	115.0	0.040	Freeze drying	470 (N_2)	7
F-PI/rGO/Co[a]	97.8% (50% strain)	146.1	~	Freeze drying	~	7
PI	90.67% (50% strain)	~	~	Freeze drying	551 (N_2)	7
PI/rGO	94.16% (50% strain)	~	~	Freeze drying	~	7
SiO_2/PI-1	possessed elasticity (80% strain)	120.0	0.041	Freeze drying	542 (air)	8
SiO_2/PI-3	Inelastic	125.0	0.0311	Freeze drying	542 (air)	8
PI/CNT	excellent recoverability (80% strain)	~	~	Freeze drying	543 (N_2)	9
PI/SAp-80	Inelastic	148.0	0.029	Supercritical drying	550 (N_2)	10
PI (sample 8)	Inelastic	147±2	0.0325	Supercritical drying	500 (N_2)	11
PI/PGG	Inelastic	80-90	~	Supercritical drying	425 (N_2)	12
PIA	Inelastic	135.0	~	Supercritical drying	442(N_2)	13
SiO_2/PI-2	98.78% (80% strain)	144.5	0.0368	Freeze drying	533.2(air)	This work
SiO_2/PI-10	99.20% (80% strain)	150.6	0.0374	Freeze drying	542.9 (air)	
SiO_2/PI-30	98.93% (80% strain)	153.1	0.0376	Freeze drying	539.1 (air)	
SiO_2/PI-D	83.43% (80% strain)	152.5	0.0371	Freeze drying	538.0 (air)	
SiO_2/PI-ND	92.52% (80% strain)	141.5	0.0383	Freeze drying	544.2 (air)	

[a] Modified with trichloro (1H,1H,2H,2H-tridecafluoro-n-octyl)silane by a chemical deposition process.

* The decomposition temperature (T_d) in nitrogen is slightly higher than that in air.

REFERENCES

1 Z. C. Qian, Z. Wang, Y. Chen, S. R. Tong, M. F. Ge, N. Zhao and J. Xu, Superelastic and ultralight polyimide aerogels as thermal insulators and particulate air filters. *J. Mater. Chem. A*, 2018, **6**, 828-832.

2 Z. Zhang, X. D. Wang, G. Q. Zu, K. Kanamori, K. Nakanishi and J. Shen, Resilient, fire-retardant and mechanically strong polyimide-polyvinylpolymethylsiloxane composite aerogel prepared via stepwise chemical liquid deposition. *Mater. Des.*, 2019, **183**, 108096.

3 H. Liu, X. Y. Chen, Y. J. Zheng, D. B. Zhang, Y. Zhao, C. F. Wang, C. F. Pan, C. T. Liu and C. Y. Shen, Lightweight, superelastic, and hydrophobic polyimide nanofiber /mxene composite aerogel for wearable piezoresistive sensor and oil/water separation applications. *Adv. Funct. Mater.*, 2021, **31**, 2008006.

4 Y. N. Wang, Q. Y. Ge, X. L. Chen, S. L. Qi, G. F. Tian and D. Z. Wu, Ultralight and flexible MWNTs/polyimide hybrid aerogels for elastic conductors. *Macromol. Mater. Eng.*, 2017, **302**, 1700082.

5 J. Liu, H. B. Zhang, X. Xie, R. Yang, Z. S. Liu, Y. F. Liu and Z. Z. Yu, Multifunctional, superelastic, and lightweight MXene/polyimide aerogels. *Small*, 2018, **14**, 1802479.

6 X. Zhao, W. L. Wang, Z. Wang, J. N. Wang, T. Huang, J. Dong and Q. H. Zhang, Flexible PEDOT:PSS/polyimide aerogels with linearly responsive and stable properties for piezoresistive sensor applications. *Chem. Eng. J.*, 2020, **395**, 125115.

7 X. Zhang, W. Li, P. Song, B. You and G. Sun, Double-cross-linking strategy for preparing flexible, robust, and multifunctional polyimide aerogel. *Chem. Eng. J.*, 2020, **381**, 122784-122784.

8 X. H. Zhang, X. X. Ni, C. X. Li, B. You and G. Sun, Co-gel strategy for preparing hierarchically porous silica/polyimide nanocomposite aerogel with thermal insulation and flame retardancy. *J. Mater. Chem. A*, 2020, **8**, 9701-9712.

9 X. Chen, H. Liu, Y. Zheng, Y. Zhai, X. Liu, C. Liu, L. Mi, Z. Guo and C. Shen, Highly Compressible and Robust Polyimide/Carbon Nanotube Composite Aerogel for High-Performance Wearable Pressure Sensor. *ACS Appl. Mater. Interfaces*, 2019, **11**, 42594-42606.

10 S. A. Wu, A. Du, Y. L. Xiang, M. F. Liu, T. M. Li, J. Shen, Z. H. Zhang, C. H. Li and B. Zhou, Silica-aerogel-powders "jammed" polyimide aerogels with excellent hydrophobicity and conversion to ultra-light polyimide aerogel. *Rsc Adv.*, 2016, **6**, 58268-58278.

11 X. Li, J. Wang, Y. Zhao and X. Zhang, Template-free self-assembly of fluorine-free hydrophobic polyimide aerogels with lotus or petal effect. *ACS Appl. Mater. Interfaces*, 2018, **10**, 16901-16910.

12 M. A. B. Meador, M. Agnello, L. McCorkle, S. L. Vivod and N. Wilmoth, Moisture-resistant polyimide aerogels containing propylene oxide links in the backbone. *ACS Appl. Mater. Interfaces*, 2016, **8**, 29073-29079.

13 D. Shen, J. Liu, H. Yang and S. Yang, Intrinsically highly hydrophobic semi-alicyclic fluorinated polyimide aerogel with ultralow dielectric constants. *Chem. Let.*, 2013, **42**, 1230-1232.